Available online at www.sciencedirect.com
SCIENCE DIRECT
Catalysis Today 106 (2005) 206–210
CATALYSIS TODAY
www.elsevier.com/locate/cattod

A novel composite support for hydrotreating catalyst aimed at ultra-clean fuels

Baojian Shen [a,*], Huifeng Li [a], Wencheng Zhang [b], Ye Zhao [b], Zhihua Zhang [b], Xiaohua Wang [a], Shikong Shen [a]

[a] *State Key Laboratory of Heavy Oil Processing, The Key Laboratory of Catalysis of CNPC, Faculty of Chemical Sciences and Engineering, University of Petroleum, Beijing, Changping 102249, China*
[b] *Research Institute of Daqing Petrochemical Company/PetroChina, Daqing 163714, China*

Available online 22 August 2005

Abstract

To produce ultra-clean fuel, a well-designed composite support, the unique combination of titanosilicate ETS-10 and aluminophosphate $AlPO_4$-5 with alumina, was firstly developed. Compared with pure alumina, it owns a certain amount of B type acid sites of moderate acid strength, contributing to the removal of refractory 4,6-DMDBT effectively. Moreover, it can impede inactive nickel spinel formation, improve metal–support interactions and favor more polymeric tungsten species formation, which facilitates the promotion effect of nickel on tungsten. With FCC diesel (sulfur: 960.0 $\mu g\ g^{-1}$ and aromatics: 51.0 vol.%) as feed, the clean diesel product (sulfur: 2.7 $\mu g\ g^{-1}$ and aromatics: 15.0 vol.%) without much over-cracking fractions, can be obtained over the composite support based catalyst, at 8.0 MPa, 633 K, LHSV of 1 h^{-1}, H_2/oil ratio of 500 (v/v).

Keywords: Titanosilicate; ETS-10; Aluminophosphate; $AlPO_4$-5; Composite support; Alumina; Metal–support interactions; Hydrodesulfurization; Aromatic hydrogenation

1. Introduction

Clean fuels production as an important subject of environmental catalysis has received considerable attention in recent years. However, it is really a big challenge for conventional hydrotreating catalysts to produce clean fuels, particularly ultra-clean diesel with lower sulfur and aromatics, according with the stringent fuel specifications. Therefore, it is imperative to develop new hydrotreating catalysts of higher activity and selectivity in hydrodesulfurization (HDS) and hydrodearomatization (HDA) [1–6].

In order to achieve this goal, many approaches have been used [1,7–9], however, novel support design is an important and practical one, because the nature of the support plays an important role in the catalyst activity [2–4]. So far, various materials have been tried as supports to load Mo or W active components promoted by Co or Ni. Some of them exhibit outstanding catalytic performances, such as the catalysts containing titania show easier reducibility or sulfidability [3,10], phosphorous modified alumina can influence the structure and dispersion of the metal oxides due to the formation of surface $AlPO_4$-like species [11,12]; besides, the incorporation of acidic molecular sieves can also enhance the activity in HDS [4,10]. However, TiO_2 owns low surface area and limited thermal stability [3,10], conventional phosphorous modification causes surface area loss or pore blocking unavoidably [11,12] and improperly controlled acidity of molecular sieves results in undesired cracking or deactivation [4,10].

Here, we would like to report our well-designed composite support, with an aim to take advantage of favorable characteristics of the above-mentioned systems but overcome their corresponding disadvantages. In this composite support, ammonium-exchanged ETS-10 of good thermal stability [13–15] and $AlPO_4$-5 of crystalline $AlPO_4$

* Corresponding author. Tel.: +86 10 89 73 33 69; fax: +86 10 89 73 33 69.
E-mail address: baojian@cup.edu.cn (B. Shen).

0920-5861/$ – see front matter © 2005 Elsevier B.V. All rights reserved.
doi:10.1016/j.cattod.2005.07.125

structure [16] are incorporated simultaneously into the alumina matrix.

The aim of present work is to investigate the effects of the introduction of ETS-10 and $AlPO_4$-5 into alumina matrix, the impact of their unique crystalline titanosilicate and aluminophosphate framework on metal–support interactions and hydrotreating performance.

2. Experimental

In a typical composite support preparation, the even mixture of ammonium-exchanged ETS-10 [15], $AlPO_4$-5 [16] and pseudo-boehmite powder was extruded, followed by drying at 393 K for 4 h and calcining at 823 K for 5 h. The obtained composite support was designated as ATSP. The catalysts NiW/ATSP and NiW/Al_2O_3 with the same loading of 4 wt% NiO and 27 wt% WO_3, were prepared, respectively, by pore volume co-impregnation method with an aqueous solution of ammonium metatungstate and nickel nitrate, followed by drying and calcining.

The supports and oxide form catalysts were characterized with the following characterization techniques, correspondingly. The X-ray diffraction (XRD) patterns were recorded on a SHIMADZU-6000 diffractometer, using the Cu Kα radiation at 40 kV and 30 mA. The surface area and pore volume were determined by N_2 physisorption using a Micromeritics ASAP 2020 automated system. Acid sites and acid type distribution were determined by infrared spectroscopy of chemisorbed pyridine on a MAGNA-IR560ESP FT-IR spectrometer. NH_3–TPD experiments were performed by using Quantachrome Autosorb-1. Diffuse reflectance spectra were recorded using corresponding support as reference on a Hitachi U-4100 Spectrophotometer. Laser Raman (LR) spectra were recorded on a computer-controlled Renishaw microscopic confocal Raman spectrometer, model RM2000, using the 514.5 nm line from a Spectra Physics model 165 Ar ion laser as the exciting source. The spectra shift width was typically 1 cm^{-1}, and laser source powers were ca. 4.7 mW.

The hydrotreating performance of the catalysts were evaluated in a continuous flow fixed-bed reactor, with FCC diesel as feed, under the conditions: the catalyst loading of 15 ml, 8.0 MPa, 633 K, LHSV of 1 h^{-1}, H_2/oil ratio of 500 (v/v). The catalysts were first pre-sulfided in situ with the sulfiding feed of 2 wt% CS_2 in kerosene. After steady state conditions were reached, the liquid effluents were periodically collected. Subsequently, the total sulfur content in the feed and products was measured by a LC-4 coulometric sulfur analyzer, and the sulfur compounds in the feed and products were identified by GC–PFPD analysis on a VARIAN 3800 Gas Chromatograph with a capillary column CP8772 (60 m × 0.32 mm). The total aromatic content of the feed and products was determined by the standard method of fluorescence indicator adsorption.

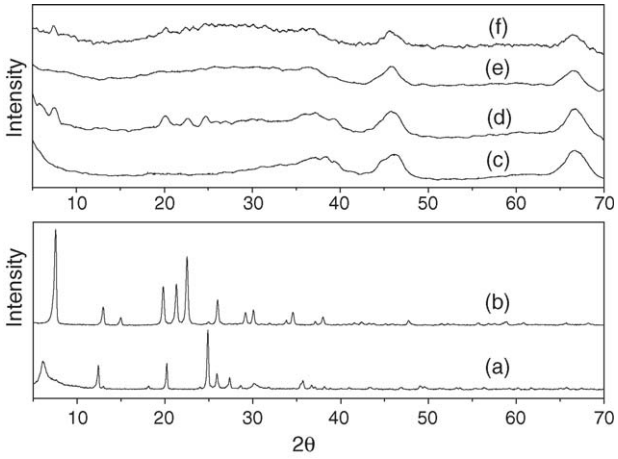

Fig. 1. XRD patterns of (a) ammonium-exchanged ETS-10, (b) $AlPO_4$-5, (c) Al_2O_3, (d) ATSP, (e) NiW/Al_2O_3 and (f) NiW/ATSP.

3. Results and discussion

3.1. X-ray diffraction

The XRD patterns of ammonium-exchanged ETS-10 and $AlPO_4$-5 after calcination at 823 K for 5 h were shown in Fig. 1, indicating both ETS-10 and $AlPO_4$-5 have good thermal stability. The XRD patterns of composite support ATSP, prepared by the incorporation ETS-10 and $AlPO_4$-5 into alumina, exhibit some additional peaks characteristic of ETS-10 and $AlPO_4$-5, compared with those of pure alumina, proving their stable embedding in the alumina matrix. After the impregnation of nickel and tungsten, no obvious metal oxides peaks are found in the XRD patterns of NiW/Al_2O_3 and NiW/ATSP, although the characteristic peaks of ETS-10 and $AlPO_4$-5 weaken to some extent, due to the dilution effect or partial breakdown of ETS-10 and $AlPO_4$-5 structure caused by the metal oxides [17,18].

3.2. N_2 physisorption

The textural properties of the samples listed in Table 1 indicate the composite support ATSP owns equivalent surface area but slightly lower total volume compared with Al_2O_3. But the surface area and pore volume of NiW/ATSP are smaller than those of NiW/Al_2O_3, correspondingly, maybe due to partial blocking or breakdown of the cavities of ETS-10 and $AlPO_4$-5 caused by metal oxides [17,18].

Table 1
BET surface areas and pore volumes of the samples

Sample	Surface area ($m^2\ g^{-1}$)	Pore volume ($cm^3\ g^{-1}$)
Al_2O_3	281	0.54
ATSP	277	0.53
NiW/Al_2O_3	193	0.36
NiW/ATSP	176	0.32

Table 2
Total acid and acid type distribution of Al_2O_3, ETS-10 and $AlPO_4$-5

Sample	473 K		623 K	
	B acid (μmol g^{-1})	L acid (μmol g^{-1})	B acid (μmol g^{-1})	L acid (μmol g^{-1})
Al_2O_3	–	313.58	–	128.40
ETS-10	30.91	541.98	–	11.11
$AlPO_4$-5	21.82	58.02	10.91	30.86
ATSP	20.00	170.37	3.64	56.79

3.3. Infrared spectroscopy

The results of the acid sites and acid type distribution of Al_2O_3, $AlPO_4$-5 and ammonium-exchanged ETS-10 were shown in Table 2, which is quite different from the earlier reported acidic molecular sieves [2,4,19,20]. It is clear that both ETS-10 and $AlPO_4$-5 own less strong-strength L type acid sites (pyridine desorption temperature at 623 K) than Al_2O_3. However, there are a certain amount of B type acid sites (pyridine desorption temperature at 473 K) existing on the surface of ETS-10 and $AlPO_4$-5, especially, still some strong-strength B type acid sites on the surface of $AlPO_4$-5, facilitating the isomerization of 4,6-DMDBT into more reactive compounds so as to enhance the HDS activity, or naphthenic rings opening through mild cracking, but avoid over-cracking or deactivation effectively [2,4,19,20].

3.4. Temperature-programmed desorption

NH_3–TPD of the supports and the oxide form catalysts were shown in Fig. 2. It was obvious that the shapes of the corresponding desorption curves were very similar, suggesting similar distributions of acidic sites over the supports or catalysts. In contrast, the NH_3 desorption peaks of the composite support ATSP or NiW/ATSP shift to lower temperature slightly in comparison with those of Al_2O_3 counterparts, ascribed to the composite support ATSP owning less total strong-strength acid sites compared with Al_2O_3, which has been proven by the results of pyridine–IR

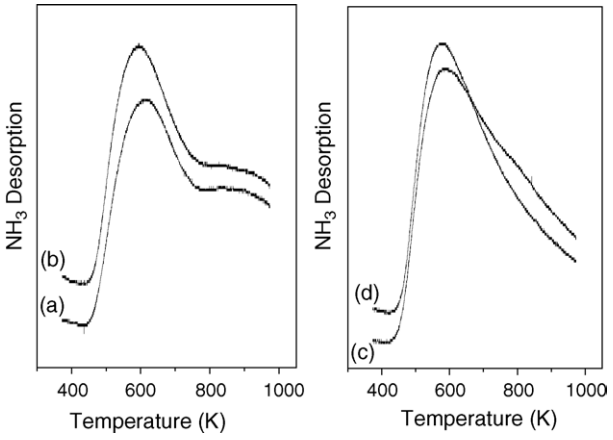

Fig. 2. NH_3–TPD spectra of (a) Al_2O_3, (b) ATSP, (c) NiW/Al_2O_3 and (d) NiW/ATSP.

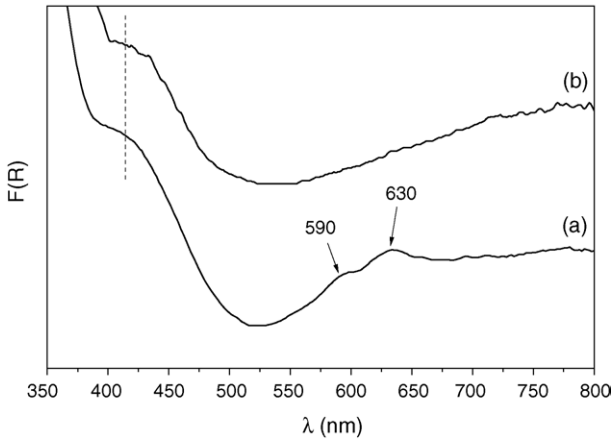

Fig. 3. DRS spectra of (a) NiW/Al_2O_3 and (b) NiW/ATSP.

desorption in Table 2. The NH_3–TPD experimental results further confirm that the composite support ATSP containing $AlPO_4$-5 and ETS-10, or its catalyst, unlike previously reported acidic molecular sieves [2,4,19,20], will not cause over-cracking.

3.5. Diffuse reflectance spectra

As the diffuse reflectance spectra (DRS) shown in Fig. 3, two visible peaks at 590 and 630 nm, are found, respectively, ascribed to the presence of tetrahedrally coordinated Ni^{2+} ions in $NiAl_2O_4$ in the spectra of NiW/Al_2O_3, consistent with the previous results [21,22]. In contrast, no such obvious peaks exist in the spectra of NiW/ATSP. But it can be clearly seen that the band around 420 nm, characteristic of octahedrally coordinated Ni^{2+} ions, shifts to higher wavenumbers with the introduction of $AlPO_4$-5 and ETS-10 into alumina, indicating an enhanced incorporation of nickel with tungsten producing Ni–W–O species. Additionally, it can be safely concluded that the Ni^{2+} ions are liable to be octahedrally coordinated on the composite support ATSP due to the modifying effects of titanosilicate framework of

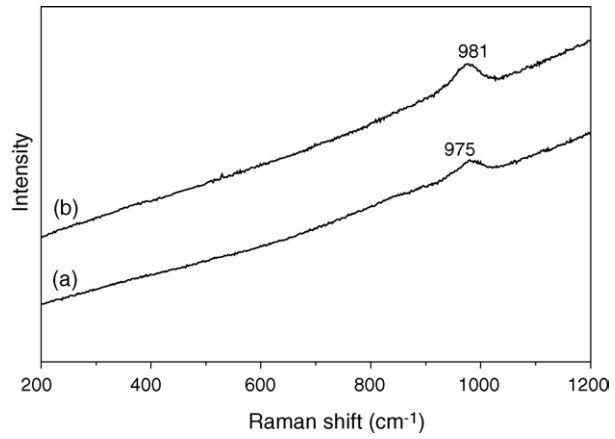

Fig. 4. Laser Raman spectra of (a) NiW/Al_2O_3 and (b) NiW/ATSP.

Table 3
The hydrotreating evaluation results

Operation conditions	Sample	Sulfur ($\mu g\ g^{-1}$)	Aromatic content (vol.%)
8.0 MPa, 633 K, LHSV of 1 h^{-1}, H_2/oil ratio of 500 (v/v)	FCC diesel feed	960.0	51.0
	Diesel product obtained over NiW/Al_2O_3	25.6	22.3
	Diesel product obtained over NiW/ATSP	2.7	15.0

ETS-10 and aluminophosphate framework of $AlPO_4$-5 on alumina, which effectively impedes the diffusion of Ni ions into the alumina lattice [21,22].

3.6. Laser Raman spectra

The LR spectra of the oxide form catalysts were shown in Fig. 4. In the LR spectra of NiW/Al_2O_3, a noticeable band at 975 cm^{-1} was found. However, the corresponding peak shifted to 981 cm^{-1} in the LR spectra of NiW/ATSP, indicating that the degree of polymerization of tungsten species is increased [23–25]. It could be ascribed to the surface characteristic of composite support ATSP favoring the formation of octahedrally coordinated polymeric tungsten species, which has been reported to interact with support weakly, probably contributing to easier reducibility and higher activity [23–26].

3.7. Catalytic activity evaluation

The hydrotreating evaluation results shown in Table 3 indicate that NiW/ATSP owns remarkably better HDS and HDA performance compared with NiW/Al_2O_3, with FCC diesel (sulfur: 960.0 $\mu g\ g^{-1}$ and aromatics: 51.0 vol.%) as feed, the ultra-low sulfur diesel product (sulfur: 2.7 $\mu g\ g^{-1}$) is obtained over NiW/ATSP, without much over-cracking fractions (because the initial boiling point of the diesel product does not shift to lower temperature and total diesel yield almost equals to 100%). In contrast, the diesel product (sulfur: 25.6 $\mu g\ g^{-1}$) is obtained over NiW/Al_2O_3 and its GC–PFPD analysis results also suggest almost half of 4,6-DMDBT in the FCC diesel feed, are left intact in the diesel product. However, no such steric-hindered refractory sulfur compounds are detectable in the diesel product obtained over NiW/ATSP, which can be partly attributed to the presence of a certain amount of B type acid sites of moderate acid strength on ATSP promoting the HDS activity [2,4,19,20]. Moreover, NiW/ATSP owns higher aromatic hydrogenation activity, reducing the aromatic content from 51.0 to 15.0 vol.%, while the diesel product (aromatics: 22.3 vol.%) is obtained over NiW/Al_2O_3. It can be explained that, firstly, the impeding formation of inactive nickel spinel as proved by DRS spectra in Fig. 3, favors the promotion effect of nickel on tungsten; secondly, the increased degree of polymerization of tungsten species as characterized by LR spectra in Fig. 4, according to the results reported by the previous literature, maybe were easier to form higher stacking number of WS_2, which can provide a higher density of multivacancies compared with single layered or thin slabs and facilitate π-complexation of the aromatic ring on such multilayered WS_2 slabs, leading to higher aromatic hydrogenation activity [25,27].

4. Conclusions

NiW/ATSP exhibits markedly higher HDS and HDA activity in hydrotreating of FCC diesel compared with NiW/Al_2O_3. It can be reasonably attributed to the advantages arising from the combination of ETS-10 and $AlPO_4$-5 with alumina. Firstly, the introduction of a certain amount of B type acid sites of moderate acid strength into Al_2O_3, could increase the HDS activity, to some extent, without causing over-cracking or severe deactivation. Secondly, it impedes inactive nickel spinel formation effectively, facilitating the promotion effect of nickel on tungsten. Thirdly, it improves metal–support interactions and favors more polymeric tungsten species formation, which maybe were easier to form higher stacking number of WS_2, leading to higher aromatic hydrogenation activity.

Acknowledgments

The authors gratefully acknowledge the funding of this project by PetroChina, NSFC (ID 20276039) and MOST "973" Project of China (2004CB217806).

References

[1] C. Song, X. Ma, Appl. Catal. B 41 (2003) 207.
[2] M. Breysse, P. Afanasiev, C. Geantet, M. Vrinat, Catal. Today 86 (2003) 5.
[3] G.M. Dhar, B.N. Srinivas, M.S. Rana, M. Kumar, S.K. Maity, Catal. Today 86 (2003) 45.
[4] G. Pérot, Catal. Today 86 (2003) 111.
[5] A. Stanislaus, B.H. Cooper, Catal. Rev. Sci. Eng. 36 (1994) 75.
[6] P.T. Vasudevan, J.L.G. Fierro, Catal. Rev. Sci. Eng. 38 (1996) 161.
[7] A.J. Hernández-Maldonado, R.T. Yang, J. Am. Chem. Soc. 126 (2004) 992.
[8] R.T. Yang, A.J. Hernández-Maldonado, F.H. Yang, Science 301 (2003) 79.
[9] S.K. Bej, S.K. Maity, U.T. Turaga, Energy Fuels 18 (2004) 1227.
[10] J. Ramírez, G. Macías, L. Cedeño, A. Gutiérrez-Alejandre, R. Cuevas, P. Castillo, Catal. Today 98 (2004) 19.
[11] T. Halachev, P. Atabasova, A. Lopez Agudo, M.G. Arias, J. Ramirez, Appl. Catal. A 136 (1996) 161.

[12] P. Atanasova, T. Tabakova, Ch. Vladov, T. Halachev, A. Lopez Agudo, Appl. Catal. A 161 (1997) 105.
[13] X. Yang, J.L. Paillaud, H.F.W.J. van Breukelen, H. Kessler, E. Duprey, Microporous Mesoporous Mater. 46 (2001) 1.
[14] A. Liepold, K. Roos, W. Reschetilowski, Z. Lin, J. Rocha, A. Philippou, M.W. Anderson, Microporous Mater. 10 (1997) 211.
[15] H. Li, B. Shen, X. Wang, S. Shen, Catal. Lett. 99 (2005) 165.
[16] S.T. Wilson, Stud. Surf. Sci. Catal. 58 (1991) 137.
[17] S. Bendezú, R. Cid, J.L.G. Fierro, A.L. Agudo, Appl. Catal. A 197 (2000) 47.
[18] R. Cid, J. VillaseÑor, F. Orellana, J.L.G. Fierro, A. López Agudo, Appl. Catal. 18 (1985) 357.
[19] A. Corma, V. González-Alfaro, A.V. Orchillés, J. Catal. 200 (2001) 34.
[20] K. Sato, Y. Iwata, Y. Miki, H. Shimada, J. Catal. 186 (1999) 45.
[21] P. Atanasova, T. Halachev, Appl. Catal. A 108 (1994) 123.
[22] B. Scheffer, J.J. Heijeinga, J.A. Moulijin, J. Phys. Chem. 91 (1987) 4752.
[23] L. Salvati Jr., L.E. Makovsky, J.M. Stencel, F.R. Brown, D.M. Hercules, J. Phys. Chem. 85 (1981) 3700.
[24] A. Gutiérrez-Alejandre, J. Ramírez, G. Busca, Langmuir 14 (1998) 630.
[25] N. Kunisada, K.-H. Choi, Y. Korai, I. Mochida, K. Nakano, Appl. Catal. A 269 (2004) 43.
[26] D. Li, A. Nishijima, D.E. Morris, G.D. Guthrie, J. Catal. 188 (1999) 111.
[27] L. Vradman, M.V. Landau, M. Herskowitz, Fuel 82 (2003) 633.